Internal structure and emplacement of the Papoose Flat pluton: an integrated structural, petrographic and magnetic susceptibility study

Michel de Saint-Blanquat* CNRS - UMR 5563 Mécanismes de Transfert en Géologie, Observatoire Midi-Pyrénées / Université Paul-Sabatier, 38 rue des 36-Ponts, F-31400 Toulouse, France.

Richard D. Law Department of Geological Sciences, Virginia Tech., Blacksburg, Virginia 24061-0420, U.S.A.

Jean-Luc Bouchez UMR 5563 Mécanismes de Transfert en Géologie, Observatoire Midi-Pyrénées / Université Paul-Sabatier, 38 rue des 36-Ponts, F-31400 Toulouse, France.

Sven S. Morgan Department of Geology, Central Michigan University, Mount Pleasant, Michigan 48859, U.S.A.

Corresponding author; michel@lucid.ups-tlse.fr

DATA REPOSITORY MATERIAL

MICROSTRUCTURES WITHIN THE PLUTON

Shear sense indicators and strain-path partitioning

A domainal pattern of top to the NNW and top to the SSE shear senses is indicated by both microstructures and c-axis and a-axis fabrics within the plastically deformed and dynamically recrystallized quartz veins located in the gneissic border facies around the western part of the pluton (Fig. DR.1). A top to the SSE shear sense is dominant on the southern margin of the pluton (i.e. pluton up shear sense), whereas on the northern margin km-scale domains of top to the SSE and top to the NNW (i.e. pluton up shear sense), are recorded. Domains of symmetric fabrics, indicating approximate coaxial deformation conditions, are recorded on both the northern and southern pluton margins. In between the margins, plastically deformed quartz veins located along the pluton long axis mostly exhibit symmetric fabrics.

ANISOTROPY OF MAGNETIC SUSCEPTIBILITY

Methods

Accurately oriented specimens from 102 stations covering the whole pluton were collected using a procedure similar to that employed for paleomagnetic studies. The location of these sites is indicated in Figure DR.2. Rock cylinders, 25 mm in diameter, were cored in the field with a

portable drill and oriented using a magnetic compass. Two or three cores were drilled per station and were cut into 22 mm-long samples. 548 samples were measured (5 samples per site). Magnetic measurements were performed using a Kappabridge KLY-2, manufactured by Agico (Brno, Czech Republic). The orientation and magnitude of the three principal axes of the AMS ellipsoid, $k1 \geq k2 \geq k3$ for each sample were calculated from the bulk susceptibility data and the orientation of the sample using the ANISOFT package (Jelinek, 1977). The tensor means of the sample data within each site were computed with the program EXAMS (Saint-Blanquat, 1993), giving the bulk magnetic susceptibility magnitude of the site, the orientation and intensity of the three main susceptibility axes $K1 > K2 > K3$, and the usual intensity (P%, F%, L%) and shape (T) parameters (definitions given in caption to Table DR.1). For each site, the orientation variability was computed as the standard deviation of the angular difference between individual samples and the site mean orientation. Primary data from our AMS study of the Papoose Flat pluton are presented in Table DR.1. Averaged values incorporating all data from the magmatic (M), high-temperature solid-state (H), and medium temperature (ML) microstructural domains are given in Table DR.2. The relationship between scalar AMS parameters is presented in Figure DR.3, and the quality assessment of directional data on Figure DR.4.

Source of AMS signature

The relationship between the fabric of a rock sample and its magnetic fabric depends on the nature of the magnetic (Fe bearing) minerals, and on the textural relationships among the mineral grains (Rochette, 1987; Jover et al., 1989; Borradaile et al., 1991; Rochette et al., 1992). If a sample contains more than one magnetic mineral, then the magnetic fabric becomes a composite of two or more subfabrics. Therefore interpreting AMS data requires careful identification and characterization of all the magnetic minerals contributing to the AMS signal. In magnetite-type granites (Ishihara, 1977), like the Papoose Flat pluton, the paramagnetic contribution of Fe-Mg silicates is negligible with respect to the ferromagnetic contribution, because of the high intrinsic magnetic susceptibility of magnetite, so only the oxide minerals need to be carefully identified. It is well know in plutonic rocks, however, that oxide minerals can suffer important sub-solidus re-equilibration (Frost et al., 1988; Frost and Lindsley, 1991). Thus the status of these minerals, mainly primary versus secondary, must be determined before any quantitative kinematic interpretation of the AMS signature of a rock sample can be made. We have investigated the magnetic mineralogy of the Papoose Flat pluton through examination of polished thin sections using reflected light microscopy (15 samples), microprobe analysis (10 samples, 71 analyses), and measurement of the relationship between susceptibility and temperature (relative to known Curie temperatures for specific minerals) for seven samples spanning the whole range of magnetic susceptibilities present in the pluton.

Optical and microprobe analysis indicates that the oxide minerals are mainly magnetite, ilmenite and hematite. The oxide minerals are mainly in the form of euhedral to subhedral grains (Figs. DR.4A and DR.4B) with a grain size ranging between 50 and 500 μ (mean around 0.1-0.2mm). The grains are commonly grouped in clusters measuring less than 1-2 mm in size. The shape ratio of the individual grains ranges between 1 and 2 irrespective of the microstructural state of the rock. In contrast, the shape ratio of the grain clusters is more sensitive to solid-state strain than to individual grain shape. The clusters are always elongate parallel to the macroscopic lineation, and their shape ratios range between 1 and 3 in the pluton's magmatic core domain (Fig. DR.5A) and commonly reaches a value of 6 or more in the gneissic border facies (Fig. DR.5B). Grain boundaries within the clusters are straight - arcuate, indicating early crystallization in equilibrium with the mafic phases within the granite. Ilmenite is typically associated with magnetite in the form of smaller grains at the periphery of the main magnetite grains, suggesting granule oxy-exsolution (Buddington and Lindsley, 1964). Some larger ilmenite grains are found as isolated grains. In addition to granule oxy-exsolution textures, various patterns of exsolution and oxidation are recognizable within the oxide grains including: 1) lamellae (trellis-type) oxy-exsolution of ilmenite within magnetite, and 2) oxy-exsolution of hematite within ilmenite and magnetite, which is expressed by thin sheets of secondary hematite growing from the borders or fractures of ilmenite and magnetite grains. This second type is widespread throughout the pluton, but heterogeneously developed. No regular trend in mineral oxidation, such as increase of hematite content toward the pluton margins, has been found.

Microprobe analysis indicates that magnetite composition approaches nearly pure Fe_3O_4 throughout the pluton. All the grains analyzed contain less than 0.2% TiO_2 + Al_2O_3 + MnO + MgO (Table DR.3). Ilmenite grains have more variable compositions, even within a given sample, particular in terms of their MnO content (2 to 10%) and hematite content (from 5 to 45%). These data show that the magnetite grains are undoubtedly re-equilibrated, and that the ilmenite grains are of several origins: primary (magmatic) for the large isolated grains, and secondary (subsolidus) resulting either from high-temperature granule oxy-exsolution of titanomagnetite, or from medium to low temperature lamellae oxy-exsolution (Buddington and Lindsley, 1964; Frost et al., 1988; Frost and Lindsley, 1991).

Susceptibility versus temperature measurements for seven samples, corresponding to the whole range of susceptibilities present in the pluton (2×10^{-2} to 3×10^{-5} SI, see next section), yield Curie temperatures T_c (above which a mineral looses its magnetization) between 565 °C and 575 °C indicating control by nearly pure magnetite in all the samples. The shape of the thermomagnetic curves demonstrate that magnetite is quantitatively the dominant magnetic mineral (Figs. DR.5C and DR.5D). Even in the sample with a susceptibility less than 5.10^{-5} SI, which suggest a

paramagnetic behavior (Rochette et al., 1992), the corresponding T°/K curve demonstrates the presence of magnetite (Fig. DR.5D).

The analyses described above indicate that pure, ~100-200 micron-sized, multi-domain magnetite grains and grain clusters control the magnetic fabric of the Papoose Flat pluton, despite the presence of several other magnetic mineral phases, including ilmenite, hematite, and Fe-silicates. In the absence of other highly susceptible minerals (e.g. pyrrhotite and maghemite), the magnetic susceptibility distribution within the pluton more or less directly reflects the amount of magnetite locally present. Because hematite has a very high magnetic anisotropy, it could contribute to the rock magnetic anisotropy, but the observation that hematite is homogeneously distributed throughout the pluton indicates that the intensity and orientation of the anisotropy of magnetic susceptibility is determined by the elongation (or shape anisotropy) of magnetite grains and clusters of magnetite grains (Stacey, 1960; Khan, 1962; Uyeda et al, 1963; Ellwood and Whitney, 1980; Rochette et al., 1992, Grégoire et al., 1995, 1998). In addition, the large sizes of the magnetite grains/clusters eliminate complications due to so-called inverse fabrics (Rochette et al., 1992). From these observations we conclude that any magnetic anisotropy zonation in the pluton should be interpreted in terms of grain shape anisotropy. The preservation of primary textural relationships, i.e. euhedral and subhedral crystal shapes, during and after cooling and subsequent re-equilibration, demonstrates that the magnetic fabric should still carry kinematic information on magmatic/submagmatic emplacement-related fabrics.

REFERENCES CITED

Borradaile, G.J., Puumala, M., and Stupavsky, M., 1991, Anisotropy of complex magnetic susceptibility as an indicator of strain and petrofabric in rocks bearing sulphides: Tectonophysics, v. 202, p. 309-318.

Buddington, A.F, and Lindsley, D.H., 1964, Iron-titanium oxide minerals and synthetic equivalents: Journal of Petrology, v. 5, p. 310-357.

Ellwood, B.B., and Whitney, J.A., 1980, Magnetic fabric of the Elberton granite, northeast Georgia: Journal of Geophysical Research, v. 85, p. 1481-1486.

Frost, B.R., and Lindsley, D.H. 1991, Occurrence of iron-titanium oxides in igneous rocks: Reviews in Mineralogy, v. 25, p. 433-468.

Frost B.R., Lindsley, D.H., and Andersen, D.J., 1988, Fe-Ti oxide-silicate equilibria; assemblages with fayalitic olivine: American Mineralogist, v. 73, p. 727-740.

Grégoire, V., Darrozes, P., Gaillot, A., Nédélec, A., and Launeau, P., 1998, Magnetic grain shape fabric and distribution anisotropy vs. rock magnetic fabric: a three dimensional case study: Journal of Structural Geology, v. 20, p. 937-944.

Grégoire, V., Saint-Blanquat, M., Nédélec, A., and Bouchez, J.L., 1995, Shape anisotropy versus magnetic interactions of magnetic grains: experiments and applications to AMS in granite rocks: Geophysical Research Letters, v. 22, p. 2765-2768.

Ishihara, S., 1977, The magnetite-series and ilmenite series granitic rocks: Mining Geology, v. 27, p. 293-305.

Jelinek, V., 1977, The statistical theory of measuring anisotropy of magnetic susceptibility of rocks and its application, *Geofyzika* n.p. ed., Brno, Czech Republic, 88 pp.

Jover, O., Rochette, P., Lorand, J.P., Maeder, M., and Bouchez, J.L., 1989, Magnetic mineralogy of some granites from the French Massif Central: origin of their low-field susceptibility: Physics of the Earth and Planetary Interiors, v. 55, p. 79-92.

Khan, M.A., 1962, The anisotropy of magnetic susceptibility of some igneous and metamorphic rocks: Journal of Geophysical Research, v. 67, B7, p. 2873-2885.

Law, R.D., Morgan, S.S., Casey, M., Sylvester, A.G., and Nyman, M., 1992, The Papoose Flat pluton of eastern California: a re-assessment of its emplacement history in the light of new microstructural and crystallographic fabric observations: Transactions Royal Society Edinburgh: Earth Sciences, v. 83, p. 361-375.

Law, R.D., Sylvester, A.G., Nelson, C.A., Morgan, S.S., and Nyman, M.W., 1993, Deformation associated with emplacement of the Papoose Flat pluton, Inyo Mountains, eastern California: Geologic Overview and Field Guide, *in* Lahren, M.M., Trexler, J.H., Jr. and Spinosa, C., eds., Crustal evolution of the Great Basin and Sierra Nevada: Cordilleran/Rocky Mountain Section, Geological Society of America Guidebook, Department of Geological Sciences, University of Nevada, Reno, p. 231-261.

Peacock, S.M., 1989, Numerical constrains on rates of metamorphism, fluid production, and fluid flux during regional metamorphism: Geological Society of America Bulletin, v. 101, p. 476-485.

Rochette, P., 1987, Magnetic susceptibility of the rock matrix related to magnetic fabrics: Journal of Structural Geology, v. 9, p. 1015-1020.

Rochette, P., Jackson, M., and Aubourg, C., 1992, Rock magnetism and the interpretation of anisotropy of magnetic susceptibility: Reviews of Geophysics, v. 30, p. 209-226.

Saint-Blanquat, M., 1993, EXAMS, an Excel macro for automatic computing of AMS data. Unpublished program, Université Paul-Sabatier, Toulouse, France.

Stacey, F.D., 1960, Magnetic anisotropy of igneous rocks: Journal of Geophysical Research, v. 65, p. 2429-2442.

Uyeda, S., Fuller, M..D., Belshe, J.C., and Girdler, R.W., 1963, Anisotropy of magnetic susceptibility of rocks and minerals: Journal of Geophysical Research, v. 68, p. 279-291.

FIGURE AND TABLE CAPTIONS

Figure DR.1. Domainal variation in shear-sense within the gneissic border facies around the western part of the Papoose Flat pluton. Upward translation of the pluton (relative to wall rocks) is indicated by top to north-northwest and top to south-southeast shear senses on the north and south margins of the pluton respectively. Shear senses indicated by field criteria (S-C structures), and by microstructures and crystallographic fabrics in plastically deformed quartz veins (Law et al., 1992, 1993). For field criteria: right hand arrow pointing down indicates a top to south-southeast shear sense; right hand arrow pointing up indicates a top to north-northwest shear sense. In aureole rocks on northwest margin of pluton, folded foliation (F) in pelitic layers at 6-10 m above pluton roof displays top to the north-northwest vergence. See text for discussion.

Figure DR.2. AMS sample locations with site numbers. Details of AMS parameters at each site are given in Table DR.1. Summit of Waucoba Mountain (WM) indicated by triangle.

Figure DR.3. Relationships between scalar AMS parameters. **(A)** Anisotropy (P%) vs. susceptibility (K). **(B)** Shape parameter (T) vs. susceptibility. **(C)** Shape parameter vs. anisotropy. See text for discussion.

Figure DR.4. Quality assessment of directional AMS data. **(A)** Stereograms illustrating degree of within-site variability in degree of alignment of principal magnetic susceptibility axes. Four classes (Types 1-4) of within-site variability are distinguished. k1 - open squares, k2 - open triangles, k3 – open circles. Solid symbols: site tensor averages; K1, K2 and K3. **(B)** Frequency of Type 1–4 classes of within-site variability for the 102 stations measured. **(C)** Frequency of within-site angular standard deviation for k1 (left) and k3 (right).

Figure DR.5. Details of magnetic minerals contributing to the AMS signal. **(A)** Shape and distribution of single oxide mineral grains and clusters of grains in the magmatic domain (black grains). **(B)** Shape and distribution of single oxide mineral grains and clusters of grains in the gneissic border facies (black grains). **(C, D)** Susceptibility versus temperature plots for samples PF5 and PF20.

Table DR.1. Raw AMS data from the Papoose Flat pluton. 1000 meter universal transverse Mercator (zone 11) grid coordinate system used; type = sites coded by degree of within-site variability of principal susceptibility axes (see Fig. DR.4), 1 all samples well grouped; 2 grouped; 3 zone axis around Kmax or Kmin; 4 dispersed; micr = microstructural domain, M magmatic, H high temp. solid state, L medium to low temp. solid state. Cv% is the coefficient of variation (= 100 x standard deviation/mean value) for each parameter. The average susceptibility is given as $K=(K_1+K_2+K_3)/3$. The principal scalar parameters are the total anisotropy percentage $P\%=100(K_1/K_3-1)$, the linear anisotropy percentage $L\%=100(K_1/K_2-1)$, and the planar anisotropy percentage $F\%=100(K_2/K_3-1)$. The shape of the susceptibility ellipsoid is given by the parameter $T=[2(\ln K_2-\ln K_3)/(\ln K_1-\ln K_3)]-1$, (Jelinek, 1981); T between -1 and 0 indicates a prolate shape; T between 0 and 1 indicates an oblate shape. The orientation parameters are the foliation, which is the plane containing K1 and K2 and perpendicular to K3, the minimum principal axis of the susceptibility ellipsoid, and the lineation which is parallel to K_1, the maximum principal axis of the ellipsoid.

Table DR.2. Averaged values of AMS data from the Papoose Flat pluton incorporating all data from the magmatic (M), high-temperature solid-state (H), and medium temperature (ML) microstructural domains. K is the mean susceptibility, P% the total anisotropy percentage, F% and L% the planar and linear anisotropy percentages respectively, T the shape parameter of Jelinek (1981), and nb is the number of sites analyzed in each microstructural domain. σ and Cv% are the standard deviation and the coefficient of variation (= 100 x standard deviation/mean value) respectively for each parameter; ecmxi° is the maximum angular departure between samples and the mean of the site for Ki; and σ_{Ki} is the standard deviation of this angular departure.

Table DR.3. Microprobe analyses of representative ilmenite and magnetite grains from the Papoose Flat pluton. For location of sample sites see Figure DR.1.

Table DR.4. Results of the thermal modeling. Each row correspond to one simulation computed with the 1D finite difference program of Peacock (1989). Parameters are : T intrusion : 800°C, T solidus : 650°C, latent heat of crystallization : 100000 J kg^{-1}, conductivity : 2.65 W m^{-1} K^{-1}, specific heat : 1000 J kg^{-1} K-1, density : 2600 kg m^{-3}. N is the number of pulses, d the thickness of each pulse in meter, T_{wr} the initial wallrock temperature, t_s the complete solidification time, T_{max} the maximum temperature in the aureole near the contact, T_{1000} the temperature 1000 m from the contact at ts, ΔT the difference between T_{wr} and T_{1000}, and te_{max} is the sum of the t_s + t_{inf} (duration of infilling, taken at 5000 years) for the N associated pulses, and corresponds to the maximum duration time of emplacement.

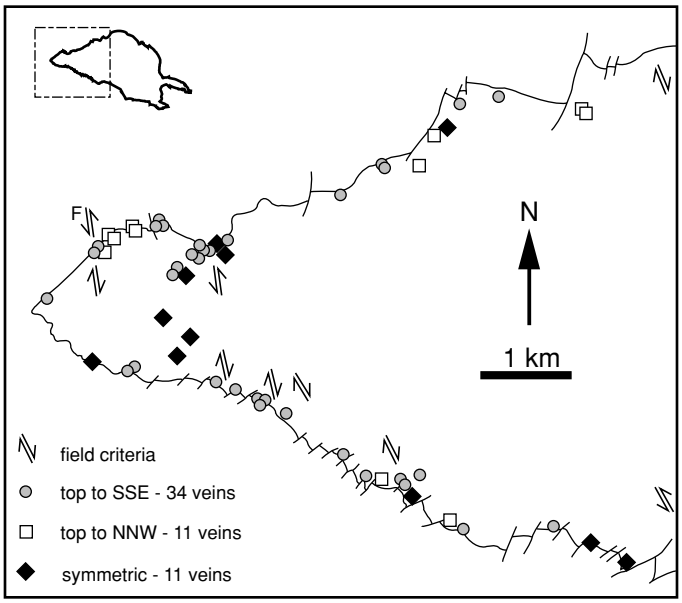
F
N
1 km
field criteria
top to SSE - 34 veins
top to NNW - 11 veins
symmetric - 11 veins

Figure DR 1

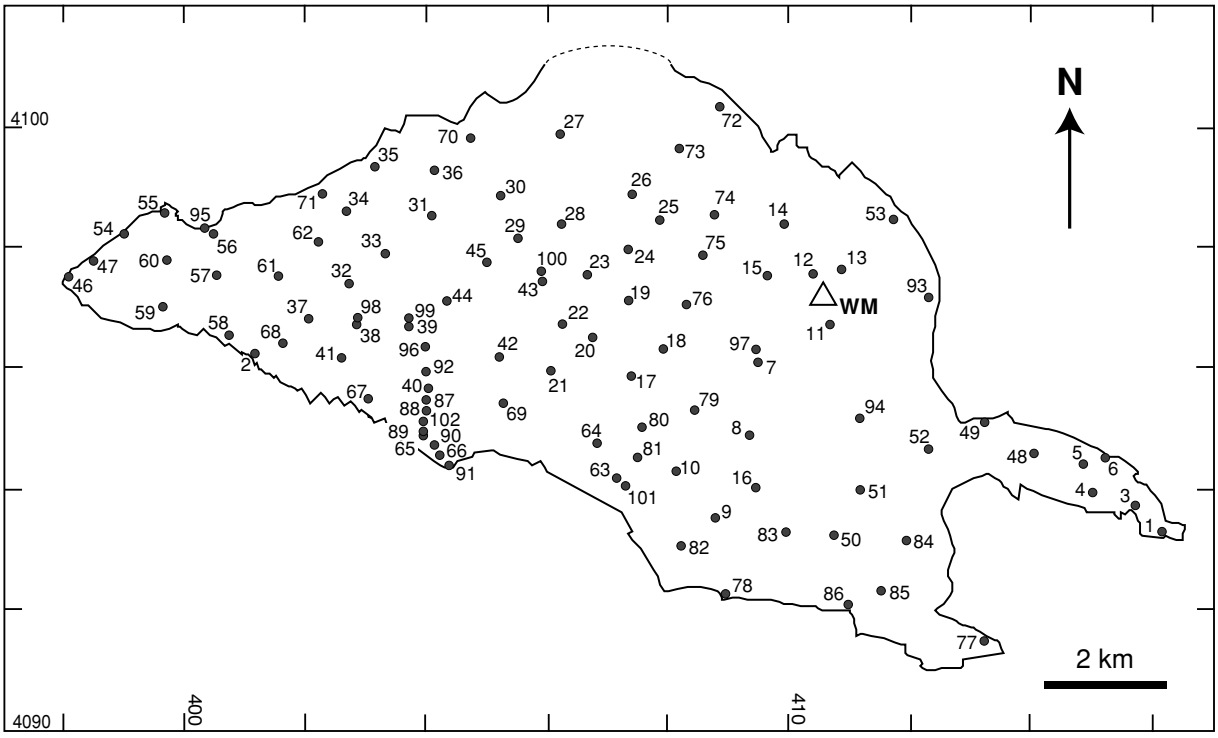

Figure DR 2

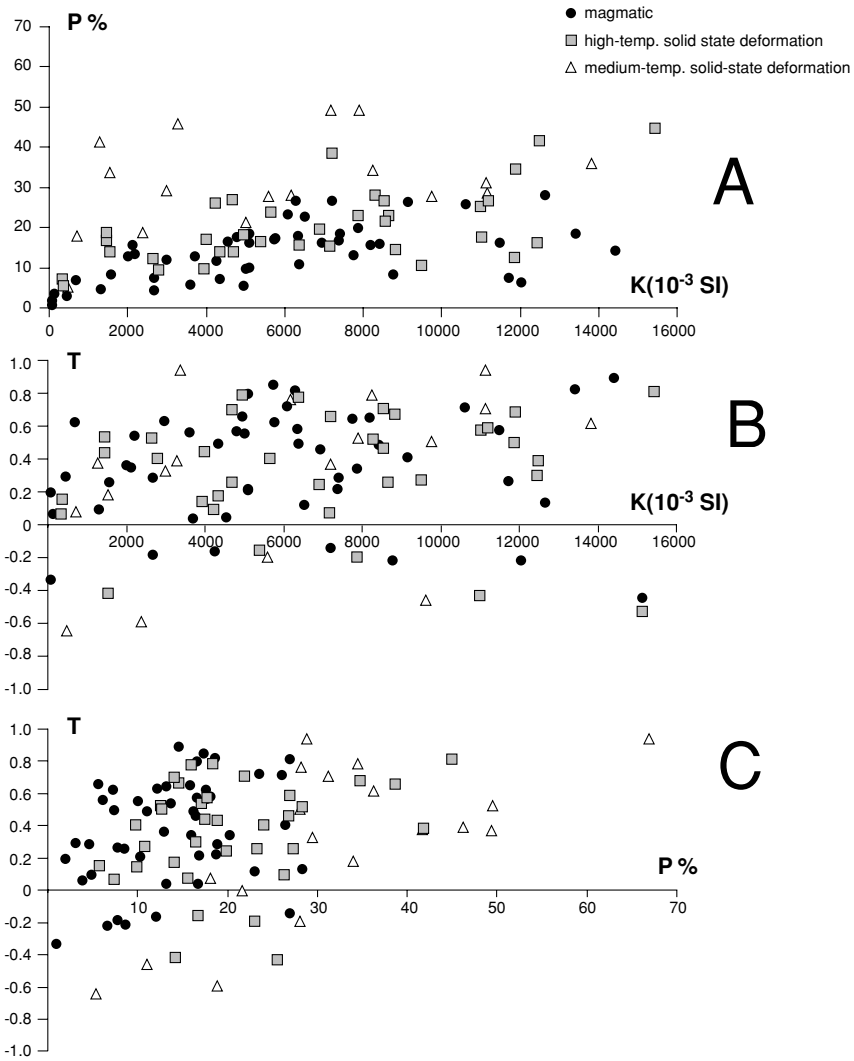
magmatic
high-temp. solid state deformation
medium-temp. solid-state deformation
P %
K(10-3 SI)
A
T
K(10-3 SI)
B
T
P %
C

Figure DR 3

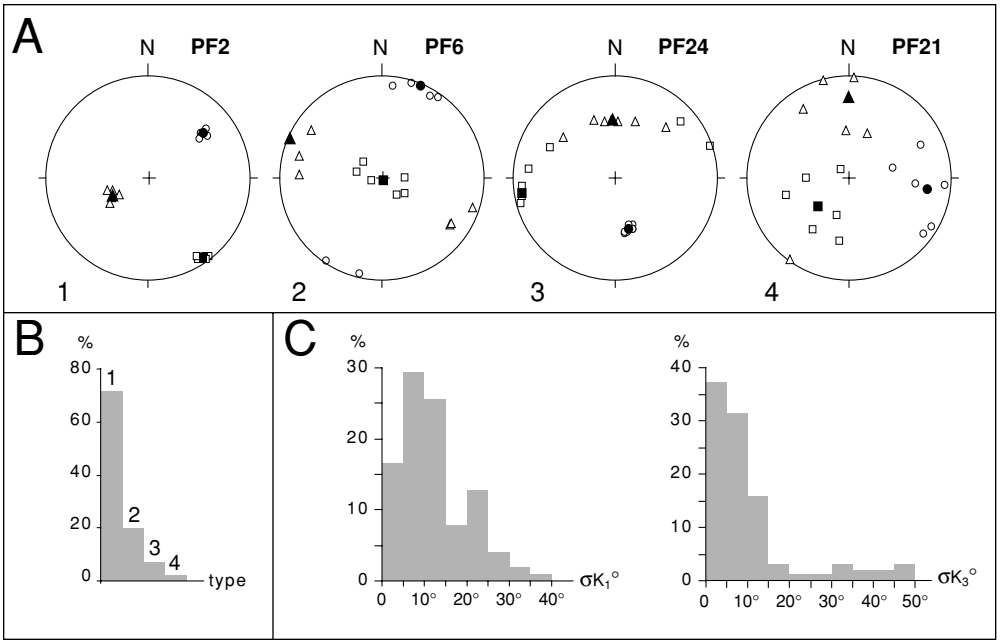
A
N
PF2
N
PF6
N
PF24
N
PF21
1
2
3
4
B
%
80
60
40
20
0
1
2
3
4
type
C
%
30
20
10
0
0
10°
20°
30°
40°
σK1°
%
40
30
20
10
0
0
10°
20°
30°
40°
50°
σK3°

Figure DR 4

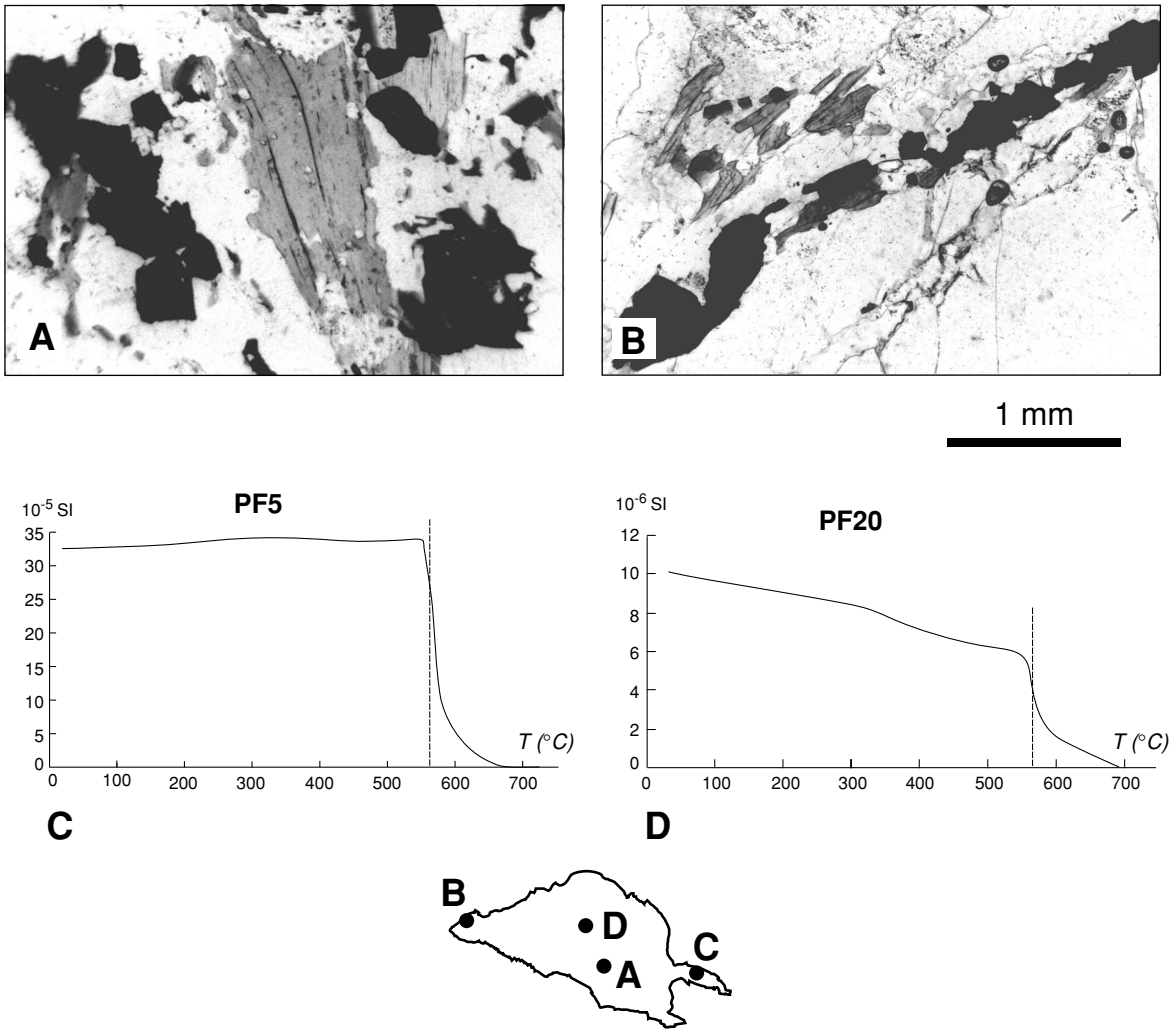
A
B
1 mm
PF5
10^{-5} SI
35
30
25
20
15
10
5
0
0
100
200
300
400
500
600
700
T (°C)
C
PF20
10^{-6} SI
12
10
8
6
4
2
0
0
100
200
300
400
500
600
700
T (°C)
D
B
D
C
A

Figure DR 5

	coordinate					susceptibility			lineation (Kmax)				foliation (plane perp. Kmin)						intensive parameters					
site	long	lat	type	micr.	nb	(10-5 SI)	σ	Cv%	trend	plunge	σ	K1(10-5SI)	Az.		Inc.	σ	K3(10-5SI)	P%	σ	Cv%	L%	F%	T
PF1	416.17	4093.30	1	M	5	1203	285	24	**182**	**57**	9	1244	**34**	**E**	**69**	49	1167	**7**	2	25	4	3	-0.22
PF2	401.15	4096.19	1	L	5	127	63	49	**145**	**6**	4	146	**141**	**W**	**59**	4	103	**42**	12	30	11	27	0.38
PF3	415.79	4093.72	1	H	5	948	89	9	**271**	**30**	11	992	**91**	**S**	**90**	2	895	**11**	4	33	4	7	0.27
PF4	415.05	4093.96	1	M	5	218	85	39	**61**	**4**	14	229	**61**	**N**	**88**	5	202	**14**	2	18	3	10	0.54
PF5	414.85	4094.44	1	M	6	155	129	84	**338**	**40**	21	160	**153**	**E**	**85**	5	148	**8**	4	42	3	5	0.26
PF6	415.24	4094.56	2	M	6	210	28	13	**151**	**88**	18	224	**113**	**S**	**87**	12	193	**16**	1	5	5	10	0.35
PF7	409.51	4096.05	3	M	3	129	42	32	**87**	**24**	9	132	**85**	**S**	**88**	22	126	**5**	1	17	2	3	0.10
PF8	409.37	4094.90	1	M	5	737	62	8	**244**	**10**	6	790	**70**	**S**	**54**	6	676	**17**	2	13	6	10	0.22
PF9	408.79	4093.52	1	H	5	1100	217	20	**249**	**53**	8	1172	**143**	**W**	**54**	4	995	**18**	1	7	3	14	0.58
PF10	408.16	4094.29	2	H	4	882	54	6	**292**	**25**	17	928	**144**	**W**	**43**	9	810	**15**	4	24	2	12	0.67
PF11	410.74	4096.70	1	L	5	1381	133	10	**341**	**38**	6	1547	**161**	**E**	**89**	3	1136	**36**	4	10	6	28	0.62
PF12	410.44	4097.57	1	L	1	1114			**275**	**73**		1206	**167**	**W**	**74**		937	**29**			1	28	0.94
PF13	410.86	4097.64	2	L	6	974	217	22	**4**	**52**	24	1074	**17**	**W**	**49**	45	838	**28**	8	29	6	20	0.51
PF14	409.96	4098.40	1	L	4	823	79	10	**311**	**27**	9	910	**125**	**N**	**80**	2	677	**34**	2	5	3	30	0.79
PF15	409.68	4097.53	1	H	5	1187	167	14	**166**	**75**	14	1321	**136**	**W**	**83**	5	980	**35**	3	10	5	29	0.69
PF16	409.46	4094.01	1	M	6	499	105	21	**215**	**12**	13	518	**96**	**S**	**14**	5	471	**10**	1	11	2	8	0.56
PF17	407.41	4095.89	4	M	5	5	2	42	**356**	**19**	31	5	**139**	**E**	**23**	36	5	**2**	2	86	1	1	0.20
PF18	407.97	4096.33	1	M	7	693	69	10	**12**	**29**	12	737	**96**	**N**	**30**	5	633	**16**	2	12	4	12	0.47
PF19	407.38	4097.11	3	M	7	818	89	11	**66**	**25**	22	865	**109**	**N**	**35**	31	747	**16**	1	8	3	13	0.65
PF20	406.77	4096.54	3	M	7	12	3	28	**273**	**3**	27	12	**93**	**N**	**78**	14	12	**4**	2	41	2	2	0.07
PF21	406.09	4095.95	4	M	6	43	20	48	**244**	**56**	38	43	**8**	**W**	**67**	26	42	**3**	2	50	1	2	0.29
PF22	406.29	4096.73	1	M	6	265	156	59	**34**	**14**	13	271	**48**	**N**	**47**	8	259	**5**	1	22	2	3	0.29
PF23	406.69	4097.56	1	M	6	775	209	27	**88**	**26**	9	812	**123**	**N**	**41**	5	718	**13**	2	16	2	11	0.65
PF24	407.34	4097.96	3	M	7	571	165	29	**261**	**7**	23	603	**75**	**N**	**43**	4	514	**17**	3	20	1	16	0.85
PF25	407.87	4098.47	1	M	6	296	118	40	**29**	**43**	7	310	**92**	**N**	**47**	4	276	**12**	2	15	2	10	0.63
PF26	407.42	4098.88	1	M	7	627	163	26	**281**	**14**	25	679	**87**	**N**	**46**	4	535	**27**	9	32	2	24	0.82
PF27	406.26	4099.88	1	H	7	398	100	25	**332**	**47**	5	425	**88**	**N**	**50**	6	362	**17**	3	19	5	12	0.45
PF28	406.25	4098.39	2	M	8	67	25	37	**284**	**4**	17	69	**103**	**N**	**46**	11	64	**7**	1	13	1	6	0.63
PF29	405.57	4098.16	1	M	5	509	201	40	**301**	**9**	10	537	**109**	**N**	**40**	5	461	**16**	5	32	2	15	0.80
PF30	405.26	4098.85	1	H	5	262	138	53	**347**	**28**	10	275	**127**	**N**	**40**	2	244	**13**	3	26	3	9	0.53
PF31	404.11	4098.54	1	M	6	576	151	26	**26**	**32**	4	612	**93**	**N**	**35**	5	521	**18**	4	24	3	14	0.63
PF32	402.71	4097.42	2	M	6	913	268	29	**347**	**46**	24	1005	**72**	**N**	**37**	49	795	**26**	11	40	7	18	0.41
PF33	403.33	4097.92	1	M	6	507	39	8	**0**	**11**	11	548	**20**	**W**	**32**	5	461	**19**	2	12	7	11	0.22
PF34	402.70	4098.59	1	M	7	424	53	12	**342**	**41**	8	449	**81**	**N**	**41**	5	401	**12**	2	13	7	5	-0.16
PF35	403.15	4099.36	1	H	8	688	163	24	**356**	**36**	12	745	**95**	**N**	**36**	8	622	**20**	3	17	7	12	0.25
PF36	404.17	4099.28	1	H	6	563	104	19	**351**	**31**	9	616	**93**	**N**	**32**	10	496	**24**	4	18	7	16	0.41
PF37	402.06	4096.82	2	H	6	536	106	20	**203**	**9**	20	580	**7**	**W**	**41**	14	497	**17**	3	19	9	7	-0.15
PF38	402.88	4096.72	1	M	6	369	36	10	**359**	**12**	6	391	**12**	**W**	**41**	4	346	**13**	1	5	6	7	0.04
PF39	403.76	4096.70	1	M	6	199	185	93	**354**	**4**	9	210	**1**	**W**	**25**	9	186	**13**	5	42	4	9	0.37
PF40	404.07	4095.70	1	M	9	651	452	69	**161**	**14**	15	717	**146**	**W**	**49**	30	583	**23**	10	43	10	12	0.12
PF41	402.61	4096.16	1	H	8	432	42	10	**166**	**10**	6	459	**159**	**W**	**60**	5	403	**14**	1	9	6	8	0.18
PF42	405.24	4096.20	1	M	7	785	143	18	**161**	**13**	13	849	**136**	**W**	**31**	10	706	**20**	4	18	6	13	0.34
PF43	405.97	4097.46	3	M	5	433	51	12	**341**	**28**	28	446	**116**	**N**	**35**	12	415	**7**	2	22	2	5	0.50
PF44	404.37	4097.12	2	M	4	265	114	43	**203**	**20**	19	275	**16**	**W**	**68**	13	256	**8**	1	16	4	3	-0.18
PF45	405.01	4097.75	2	M	4	493	61	12	**15**	**28**	21	504	**108**	**N**	**29**	12	477	**6**	1	24	1	5	0.66
PF46	398.07	4097.50	1	H	16	152	82	54	**349**	**6**	11	164	**177**	**W**	**32**	11	144	**14**	7	49	10	4	-0.42
PF47	398.55	4097.76	1	L	5	959	184	19	**354**	**12**	6	1018	**7**	**W**	**44**	11	917	**11**	2	16	8	3	-0.45
PF48	414.05	4094.59	1	M	5	876	128	15	**316**	**12**	7	915	**16**	**W**	**14**	4	842	**9**	1	13	5	3	-0.21
PF49	413.29	4095.13	1	M	6	1263	123	10	**12**	**18**	5	1415	**13**	**W**	**88**	3	1103	**28**	3	10	11	15	0.14
PF50	410.78	4093.24	1	M	6	1339	122	9	**320**	**48**	10	1420	**75**	**N**	**50**	3	1198	**19**	2	11	1	17	0.83
PF51	411.18	4094.01	1	M	6	1059	128	12	**5**	**62**	10	1151	**37**	**W**	**75**	9	913	**26**	2	9	3	22	0.72
PF52	412.32	4094.64	1	M	6	633	108	17	**14**	**15**	15	675	**19**	**W**	**76**	8	572	**18**	1	8	3	14	0.59
PF53	411.79	4098.42	1	H	4	1112	81	7	**271**	**64**	16	1225	**150**	**W**	**68**	6	934	**31**	7	23	4	26	0.71
PF54	398.98	4098.25	1	L	5	153	50	32	**345**	**11**	9	174	**12**	**W**	**23**	13	130	**34**	9	25	13	19	0.19
PF55	399.74	4098.59	2	L	6	69	29	42	**321**	**13**	22	74	**26**	**W**	**13**	7	63	**18**	10	54	8	9	0.08
PF56	400.58	4098.26	1	L	3	718	20	3	**352**	**27**	2	844	**75**	**N**	**27**	1	565	**49**	3	6	13	32	0.37
PF57	400.59	4097.53	2	L	6	47	20	42	**353**	**9**	13	48	**8**	**W**	**49**	49	46	**5**	1	15	4	1	-0.64
PF58	400.76	4096.56	1	L	4	556	156	28	**157**	**0**	4	631	**156**	**W**	**47**	7	493	**28**	2	8	16	10	-0.19
PF59	399.67	4097.01	2	L	6	238	115	48	**347**	**11**	6	263	**21**	**W**	**21**	44	221	**19**	5	27	15	4	-0.59
PF60	399.72	4097.83	1	L	4	326	69	21	**357**	**41**	9	380	**47**	**N**	**48**	11	259	**46**	2	3	12	30	0.40
PF61	401.62	4097.54	1	H	4	714	44	6	**4**	**25**	4	765	**97**	**N**	**26**	5	662	**16**	1	5	7	8	0.08
PF62	402.23	4098.10	1	M	5	509	111	22	**354**	**18**	9	532	**26**	**W**	**29**	10	483	**10**	2	20	4	6	0.21
PF63	407.31	4094.05	1	H	5	863	96	11	**267**	**55**	7	946	**173**	**W**	**55**	10	768	**23**	2	9	8	14	0.26
PF64	406.86	4094.75	1	H	5	494	78	16	**221**	**49**	13	525	**154**	**W**	**53**	11	443	**18**	2	9	2	16	0.79
PF65	404.01	4094.93	1	H	8	276	69	25	**150**	**6**	14	287	**144**	**W**	**48**	8	262	**10**	2	17	3	7	0.41
PF66	404.25	4094.57	1	L	6	616	209	34	**159**	**7**	12	671	**148**	**W**	**36**	7	524	**28**	8	29	3	24	0.77
PF67	403.08	4095.51	1	H	6	1248	129	10	**345**	**2**	5	1438	**166**	**W**	**53**	5	1014	**42**	4	10	11	27	0.39
PF68	401.63	4096.41	1	H	5	785	185	24	**155**	**13**	4	873	**145**	**W**	**55**	5	710	**23**	5	20	13	9	-0.19
PF69	405.31	4095.44	1	H	6	392	71	18	**146**	**16**	12	409	**123**	**S**	**37**	7	373	**10**	1	10	4	6	0.15
PF70	404.78	4099.82	1	H	6	828	206	25	**336**	**33**	7	912	**93**	**N**	**36**	5	711	**28**	5	16	6	21	0.52

	coordinate					susceptibility			lineation (Kmax)				foliation (plane perp. Kmin)					intensive parameters					
site	**long**	**lat**	**type**	**micr.**	**nb**	(10-5 SI)	σ	**Cv%**	**trend**	**plunge**	σ	**K1**(10-5SI)	**Az.**		**Inc.**	σ	**K3**(10-5SI)	**P%**	σ	**Cv%**	**L%**	**F%**	**T**
PF71	402.29	4098.89	1	L	9	499	60	12	**341**	**30**	5	548	**70**	**N**	**30**	10	451	**22**	3	15	10	10	0.00
PF72	408.86	4100.30	1	H	4	854	72	8	**21**	**12**	16	917	**28**	**W**	**62**	3	752	**22**	1	5	3	18	0.71
PF73	408.19	4099.64	1	H	6	635	21	3	**322**	**28**	12	669	**113**	**N**	**47**	6	578	**16**	1	9	2	14	0.78
PF74	408.80	4098.52	1	H	6	468	90	19	**230**	**1**	14	491	**50**	**N**	**51**	3	430	**14**	1	8	2	12	0.70
PF75	408.59	4097.86	1	M	6	478	194	41	**231**	**7**	13	509	**46**	**N**	**48**	5	432	**18**	4	24	4	14	0.57
PF76	408.35	4097.05	2	M	6	1146	151	13	**74**	**5**	15	1217	**80**	**N**	**35**	5	1044	**16**	3	20	3	13	0.58
PF77	413.24	4091.52	1	H	3	421	50	12	**241**	**45**	6	469	**152**	**W**	**45**	4	371	**26**	3	10	11	14	0.10
PF78	408.96	4092.29	1	H	4	1097	190	17	**245**	**18**	5	1243	**119**	**S**	**23**	15	990	**25**	3	10	18	7	-0.43
PF79	408.48	4095.34	2	M	6	1171	107	9	**257**	**49**	23	1211	**81**	**S**	**79**	35	1124	**8**	1	10	3	5	0.27
PF80	407.60	4095.06	2	M	8	842	72	9	**122**	**23**	15	894	**107**	**S**	**62**	9	770	**16**	2	12	4	12	0.49
PF81	407.52	4094.50	1	H	2	1543	563	36	**180**	**11**	13	1743	**176**	**W**	**74**	11	1202	**45**	13	28	3	40	0.82
PF82	408.22	4093.08	1	H	7	1243	59	5	**257**	**41**	8	1328	**127**	**S**	**49**	7	1140	**16**	3	17	5	10	0.30
PF83	409.95	4093.31	3	H	3	1441	77	5	**331**	**79**	29	1508	**74**	**N**	**80**	1	1317	**14**	1	5	1	14	0.90
PF84	411.96	4093.16	2	M	7	606	173	29	**328**	**55**	15	654	**77**	**N**	**57**	5	529	**23**	4	15	3	20	0.73
PF85	411.55	4092.33	2	H	5	1185	189	16	**268**	**29**	22	1244	**76**	**N**	**63**	17	1104	**13**	2	16	3	9	0.51
PF86	411.04	4092.07	1	H	3	33	4	13	**246**	**51**	6	34	**123**	**S**	**56**	6	31	**7**	0	6	3	4	0.07
PF87	404.01	4095.51	1	H	3	852	8	1	**157**	**10**	3	937	**147**	**W**	**47**	2	739	**27**	2	7	7	19	0.47
PF88	403.98	4095.36	1	H	2	720	140	19	**166**	**22**	2	809	**148**	**W**	**53**	2	584	**39**	2	5	6	31	0.66
PF89	403.98	4095.14	1	H	2	466	23	5	**155**	**27**	3	518	**119**	**S**	**41**	3	407	**27**	1	3	9	16	0.26
PF90	404.17	4094.75	1	H	2	1117	6	1	**147**	**2**	7	1223	**145**	**W**	**43**	2	964	**27**	1	2	5	21	0.60
PF91	404.40	4094.41	2	L	2	336	1	0	**306**	**38**	24	390	**1**	**W**	**43**	4	233	**67**	2	4	1	64	0.94
PF92	404.02	4095.95	1	M	3	453	48	11	**173**	**27**	4	488	**149**	**W**	**52**	5	418	**17**	2	12	8	8	0.05
PF93	412.36	4097.15	2	H	8	790	188	24	**330**	**51**	21	919	**3**	**W**	**68**	31	614	**49**	7	14	10	36	0.53
PF94	411.19	4095.19	2	M	9	637	106	17	**117**	**54**	32	665	**137**	**E**	**75**	11	598	**11**	1	10	3	8	0.50
PF95	400.51	4098.34	1	L	3	299	41	14	**338**	**30**	10	333	**84**	**N**	**30**	5	257	**29**	8	26	9	19	0.33
PF96	403.84	4096.20	1	H	7	35	5	14	**177**	**9**	8	36	**166**	**W**	**47**	8	34	**6**	1	20	2	3	0.16
PF97	409.50	4096.06	1	M	4	718	67	9	**48**	**28**	3	809	**162**	**E**	**30**	3	638	**27**	2	6	14	11	-0.14
PF98	402.87	4096.73	1	M	4	738	51	7	**21**	**11**	5	796	**61**	**N**	**18**	2	670	**19**	2	10	6	12	0.29
PF99	403.75	4096.71	2	M	2	6	0	2	**339**	**32**	5	6	**148**	**E**	**71**	17	6	**1**	0	5	1	0	-0.33
PF100	405.96	4097.47	3	M	2	359	71	20	**34**	**39**	23	368	**125**	**N**	**39**	1	347	**6**	1	12	1	5	0.57
PF101	407.30	4094.06	1	H	4	144	13	9	**233**	**62**	7	154	**176**	**W**	**67**	2	131	**17**	1	7	4	13	0.54
PF102	404.00	4094.94	1	H	3	144	10	7	**142**	**2**	2	154	**139**	**W**	**42**	2	130	**19**	3	14	5	13	0.44

Table DR 1

	susceptibility (10^{-5}SI)			anisotropy					shape	lineation				foliation					
	K	s(K)	cv(K)%	P%	s(P%)	cv(P%)%	F%	L%	T	trend	plunge	ecmx1°	s(K1)°	azimuth		dip	ecmx3°	s(K3)°	nb
M	577	111	25	14	3	20	10	4	0.36	12	26	24	15	75	N	39	19	11	47
H	677	102	16	20	3	14	15	6	0.39	343	5	14	9	158	W	43	9	7	38
ML	586	95	23	32	5	19	21	8	0.26	337	26	16	11	1	W	40	18	11	17
all	613	105	22	19	3	18	13	5	0.35	345	21	19	12	19	W	32	15	10	102

Table DR 2

site	2	51	96	2	51	96
min	Ilm	Ilm	Ilm	Mag	Mag	Mag
SiO2	0.03	0.05	0.01	0.03	0.07	0.2
TiO2	50.04	29.53	48.93	0.03	0.03	0.01
Al2O3	0	0	0	0.04	0.01	0.02
Cr2O3	0	0	0.03	0.04	0	0.04
Fe2O3(c)	4.88	44.67	6.94	69.16	68.76	68.16
FeO(c)	42.55	24.23	32.75	31.22	31.15	30.99
MnO	2.44	2.31	10.45	0.05	0	0.07
MgO	0	0.03	0	0.01	0	0
CaO	0	0	0.02			
ZnO			0.67			0.14
NiO			0.06			0
Sum Ox%	99.95	100.84	99.86	100.6	100.02	99.64
Si	0.001	0.001	0	0.001	0.003	0.008
Ti	0.953	0.568	0.933	0.001	0.001	0
Al/Al IV	0	0	0	0	0	0
Al VI	0	0	0	0.002	0	0.001
Cr	0	0	0.001	0.001	0	0.001
Fe3+	0.093	0.86	0.132	1.993	1.993	1.982
Fe2+	0.901	0.519	0.695	1	1.003	1.001
Mn2+	0.052	0.05	0.224	0.002	0	0.002
Mg	0	0.001	0	0.001	0	0
Ca	0	0	0.001			
Zn			0.012			0.004
Ni			0.001			0
Sum Cat#	2	2	2	3	3	3
Ilmenite	90.11	51.87	70.49			
Geikielite	0.01	0.1	0.01			
Pyrophanite	5.22	5.01	22.77			
Hematite	4.65	43.02	6.72			

Table DR 3

N		d	T_{wr}	T_{max}	T_{1000}	ΔT	t_s	te_{max}	
1		3000	200	477	330	130	42000	47000	a+tinf
		3000	300	533	460	160	50000	55000	b+tinf
2	a	1500	200	477	260	60	10000		
	b	1500	300	533	384	84	14000	29000	a+b+tinf
	c	1500	400	590	500	100	19000	38000	b+c+tinf
3	a	1000	200	477	328	128	4500		
	b	1000	300	533	425	125	6000		
	c	1000	400	590	440	40	9000	24500	a+b+c+tinf
	d	1000	500	642	550	50	17000	37000	b+c+d+tinf
4	a	750	200	476	203	3	2000		
	b	750	300	533	305	5	2600		
	c	750	400	590	411	11	3700	18100	a+b+c+d+tinf
	d	750	450	617	470	20	4800	20500	a+b+c+e+tinf
	e	750	500	642	525	25	7200	23300	b+c+d+e+tinf
5	a	600	200	477	201	1	1700		
	b	600	300	534	303	3	2200		
	c	600	400	590	410	10	3200		
	d	600	450	617	462	12	4200		
	e	600	500	643	523	23	6100	22400	a+b+c+d+e+tinf
6	a	500	200	479	200	0	1100		
	b	500	300	535	301	1	1500		
	c	500	400	591	403	3	2100		
	d	500	450	618	457	7	2800		
	e	500	500	644	515	15	4200		
	f	500	550	670	574	24	7500	24200	a+b+c+d+e+f+tinf

Table DR 4